Electronic Supporting Information

Tuning the Mechanical Flexibility of Organic Molecular Crystal by Polymorphism for Flexible Optical Waveguide

Torvid Feiler,[a] Biswajit Bhattacharya,*[a] Adam A. L. Michalchuk,[a] Seon-Young Rhim,[b] Vincent Schröder,[bc] Emil List-Kratochvil*[bc] and Franziska Emmerling*[ad]

a BAM Federal Institute for Materials Research and Testing, Richard-Willstätter-Str 11, 12489 Berlin, Germany

b Department of Chemistry, Department of Physics, Humboldt-Universität zu Berlin, IRIS Adlershof, Brook-Taylor-Straße 6, 12489 Berlin, Germany

c Helmholtz-Zentrum Berlin für Materialien und Energie GmbH, Brook-Taylor-Straße 6, 12489 Berlin, Germany

d Department of Chemistry, Humboldt-Universität zu Berlin, Brook-Taylor-Str. 2, 12489 Berlin, Germany

E-mail: biswajit.bhattacharya@bam.de (BB)**;** emil.list-kratochvil@hu-berlin.de (ELK) franziska.emmerling@bam.de (FE)

Table of Contents

Thermal Study

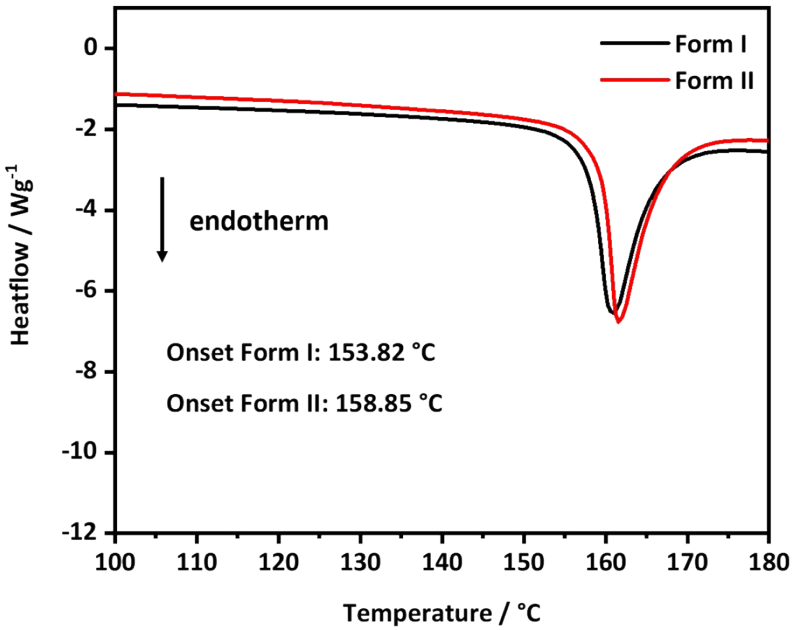

Fig. S1 Differential scanning calorimetry measurement of Form I (black line) and Form II (red line) of CPMBP.

PXRD

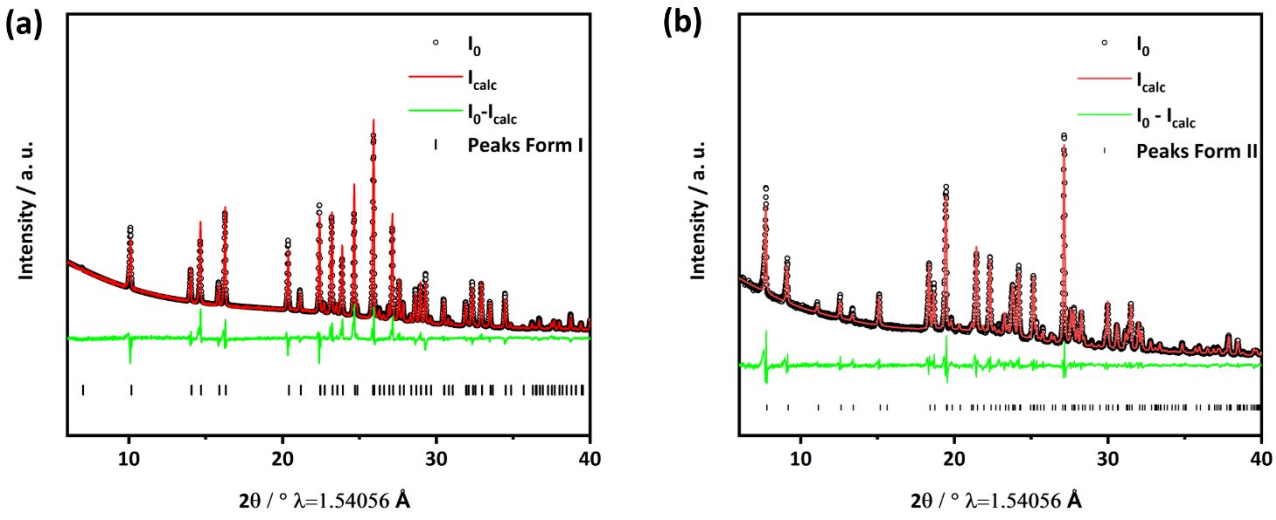

Fig S2. Rietveld refinement of (a) Form I and (b) Form II of CPMBP crystals.

ATR-IR spectroscopy

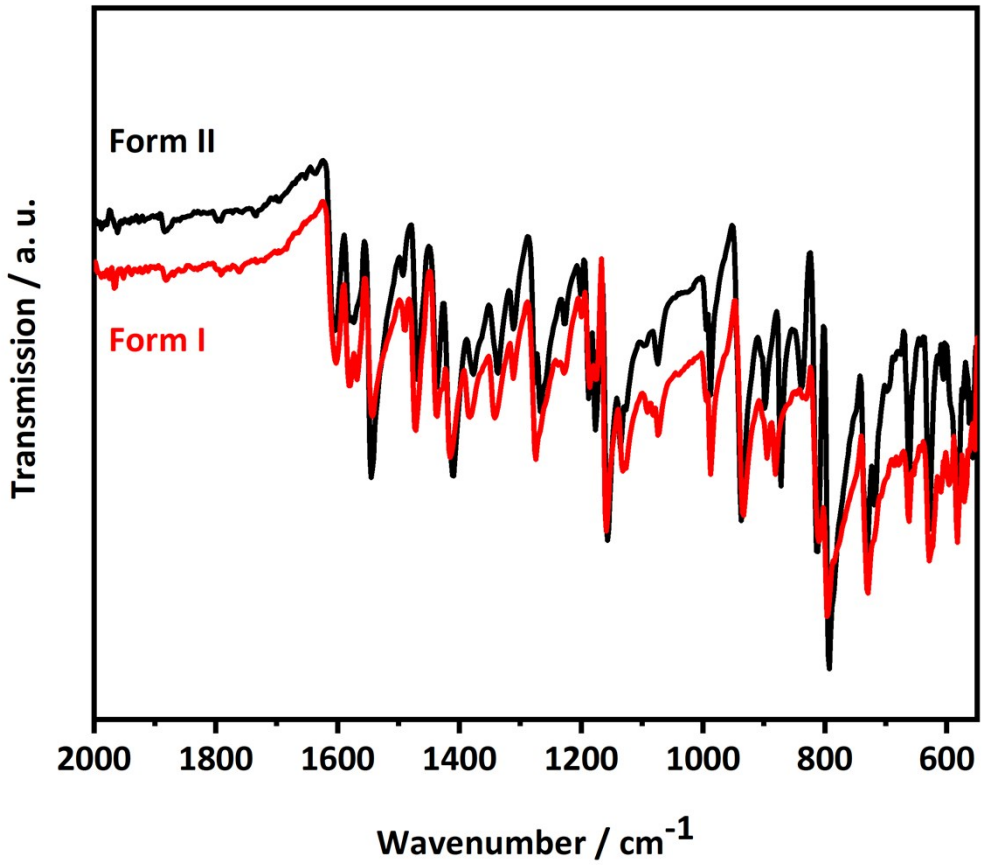

Fig. S3 FTIR spectra of Form I (red line) and Form II (black line) of CPMBP crystals.

Tables related to SCXRD

Table S1. Crystallographic and structural refinement parameters of CPMBP Form I and Form II.

Compound Name	Form I	Form II
Temperature/K	150	150
Formula	$C_{12}H_8BrClN_2O$	$C_{12}H_8BrClN_2O$
Formula Weight	311.56	311.56
Crystal System	Orthorhombic	Monoclinic
Space group	$Pca2_1$	$P2_1/c$
a/Å	25.1344(12)	4.4399(3)
b/Å	3.87360(10)	19.0147(11)
c/Å	11.9831(5)	13.8964(9)
α/ ◦	90	90
β/ ◦	90	92.184(3)
γ/ ◦	90	90
V/Å^3	1166.68	1172.14(13)
Z	4	4
Dc/g cm−3	1.774	1.765
μ/mm−1	3.735	3.717
F(000)	616	616
θ range/ ◦	2.3- 26.8	2.6- 26.8
Reflections collected	8638	7915
Unique reflections	2444	2497
Reflections $I > 2\sigma(I)$	2170	1953
Rint	0.034	0.059
Goodness of fit (F 2)	1.010	1.03
$R1$ ($I > 2\sigma$(I))	0.0238	0.0576
$wR2(I > 2\sigma$(I))	0.0510	0.1548
CCDC No.	2082068	2082067

Figures related to SCXRD

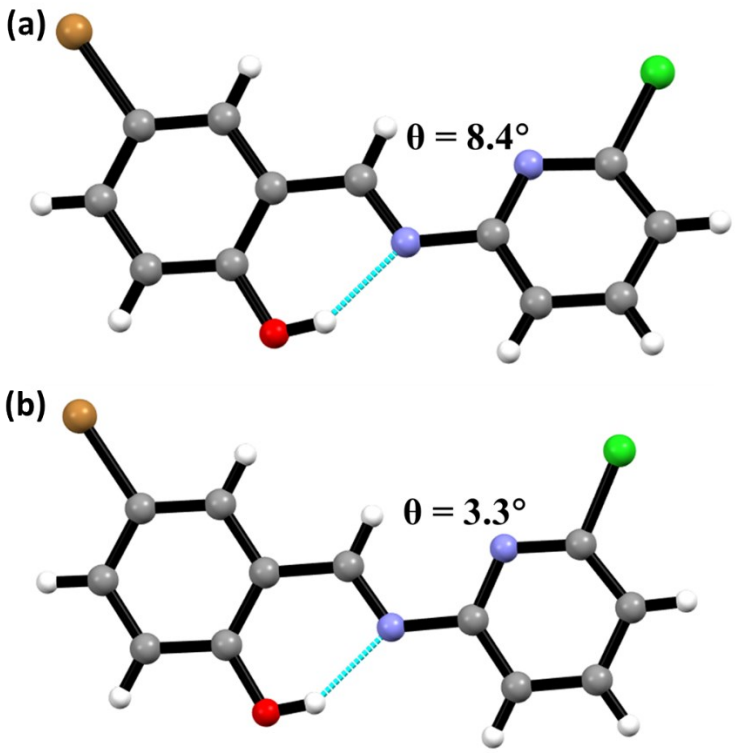

Fig S4. Molecular configuration of brittle Form I (a) and plastic Form II (b) of CPMBP crystals. Dihedral angles θ is shown in each case.

Face Indices of Crystals

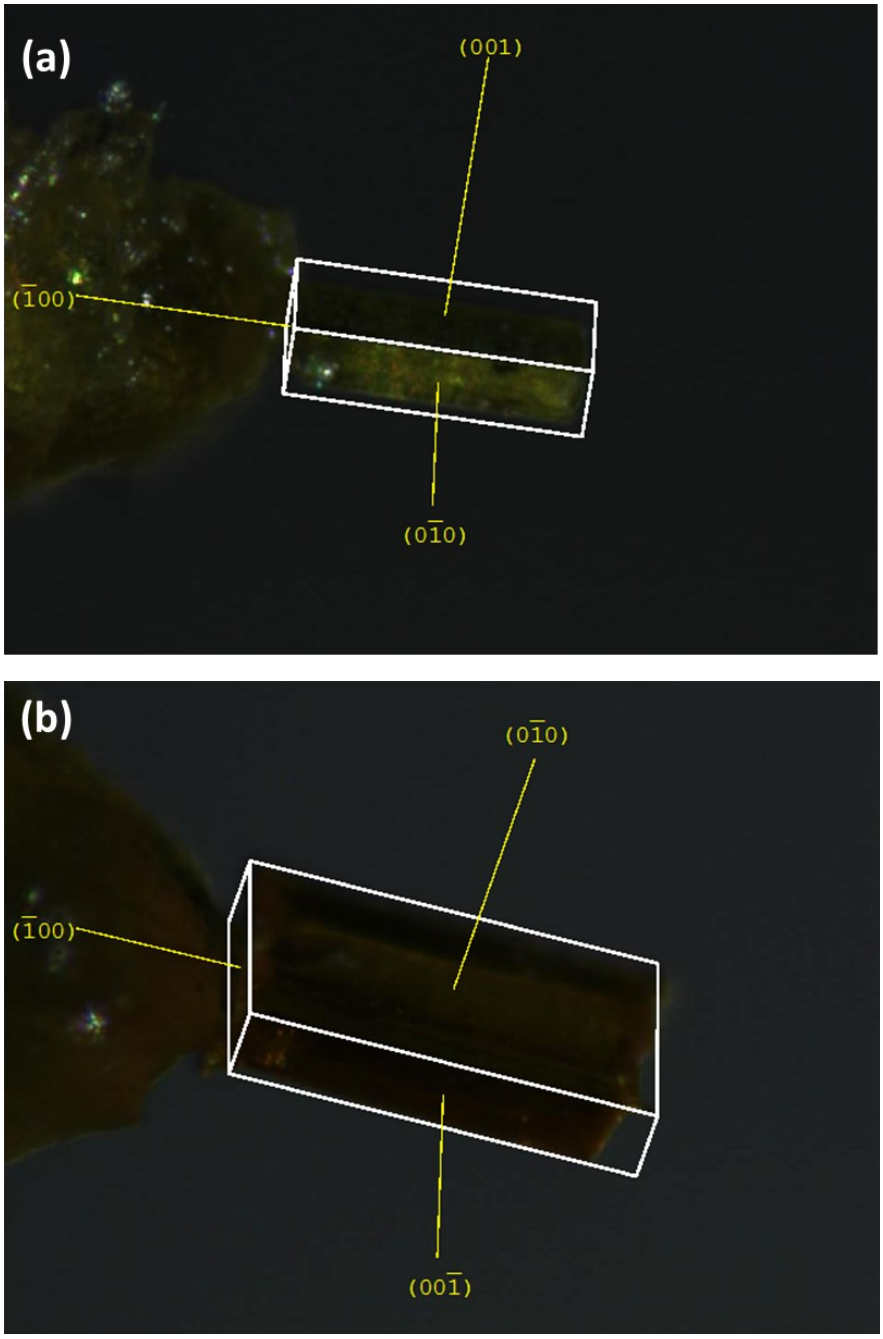

Fig. S5 Face indices image of pristine crystal of (a) Form I, and (b) Form II of CPMBP crystal.

Mechanical properties of crystals

To explore the mechanical properties of both forms of CPMBP single crystal, we conducted three-point bending experiments in which forceps restrain either end of the crystal while a needle exerts a force between them. The crystals of form I show brittle fracture when stressed on the two long crystallographic faces (001) and (010). Mechanically interlocked 3D network structure which prevents the molecules from moving in response to mechanical stress of form I is consistent with the observed brittle fracture.[1,2] The crystals of form II deformed plastically when bent on the (010) crystal face to acute angles without macroscopic fracture. In contrast, when crystals were stressed along the (001) face,

brittle fracture was observed. The existence of anisotropy in the crystal packing with low energy slip planes corroborate the plastic bending in the form II.[3]

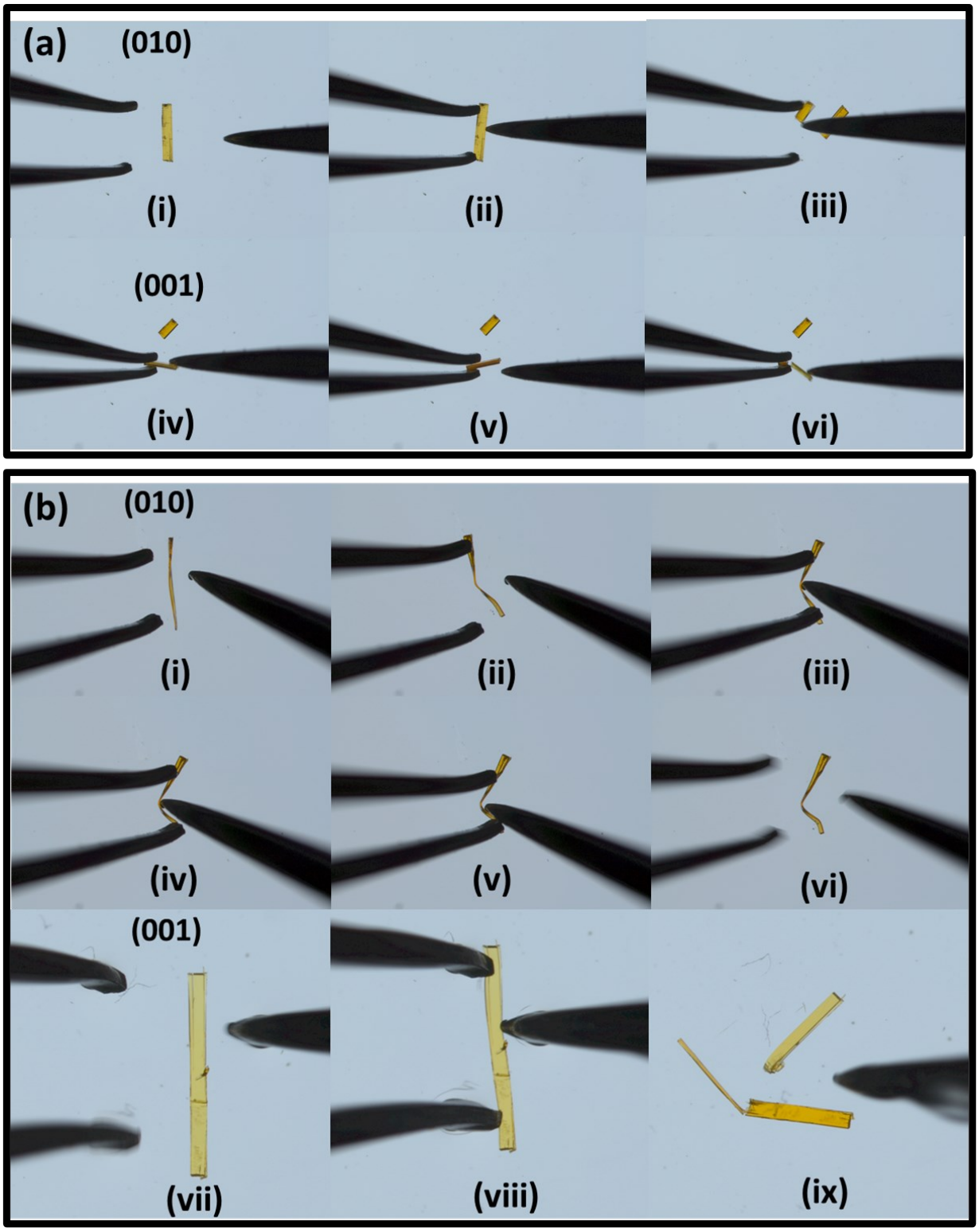

Fig. S6 Optical microscopic photographs of CPMBP crystals undergoing three-point bending experiments. (a) Brittle fracture of form I crystals over the [i-iii] (010), and [iv-vi] (001) crystallographic faces. (b) Plastic bending of form II crystals along the major crystallographic faces [i-vi] (010) and brittle fracture when stressed along the [vii-ix] (001) crystallographic face.

Hirshfeld surface analysis

Hirshfeld surface and fingerprint analyses were performed to quantitatively compare the intermolecular interactions within the asymmetric unit of both the forms of CPMBP crytsal. The plotting was based on electron distribution calculated at the B3LYP/6-31G (d,p) level of theory by using the CrystalExplorer 17.5 software.[4,5]

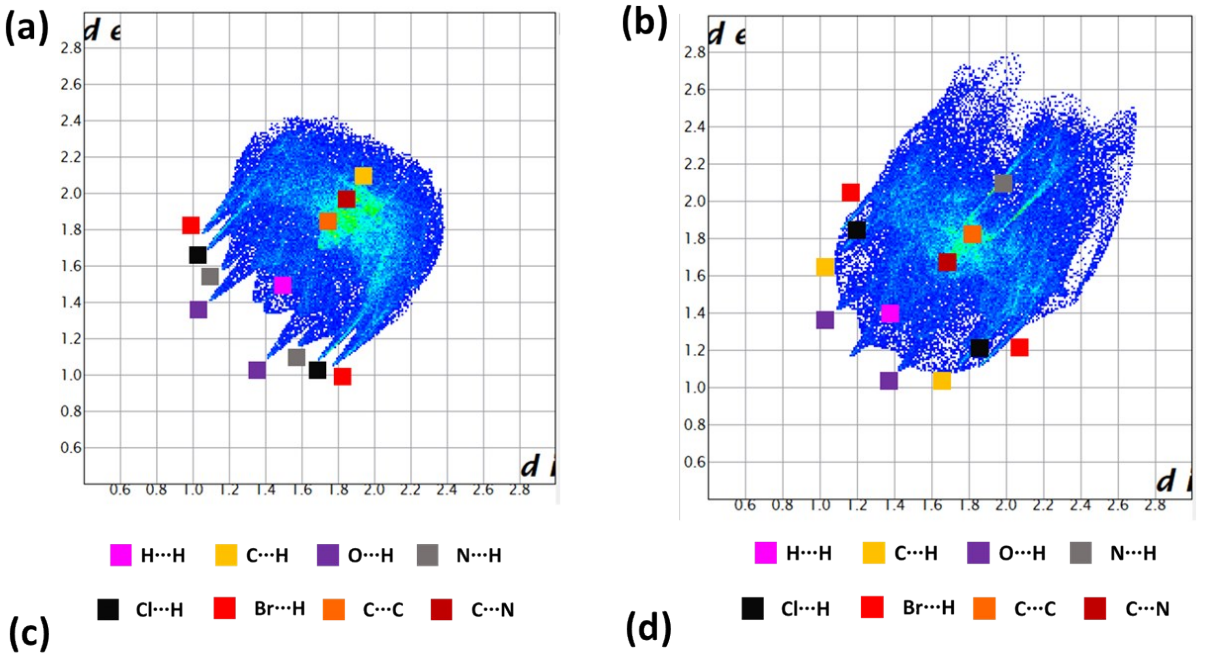

(c)

Type of Interaction	Relative contribution (%)
H....H	20.6
C....H	11.2
O....H	7.3
N....H	5.6
Cl....H	16.7
Br....H	16.8
C...C	9.6
C...N	4.7
Other	7.5

(d)

Type of Interaction	Relative contribution (%)
H....H	21.8
C....H	17.9
O....H	7.9
N....H	2.3
Cl....H	13.5
Br....H	12.3
C...C	6.5
C...N	5.8
Other	12

Fig. S7 (a, b) Two-dimensional fingerprint plots of the Hirshfeld surface, (c, d) Relative contribution to the surface for various contacts in Form I and Form II of CPMBP crystal, respectively.

CLP-PIXEL analysis

CLP-PIXEL analysis was performed on the unit cell coordinates for each of the polymorphic forms. The total lattice energy is provided in Table S2, with pairwise intermolecular energies given in Tables S3-4.

Table S2| CLP-PIXEL lattice energies for CPMBD polymorphic forms based on B3LYP/6-31G(d,p) charge densities.

Energy /kJ.mol^{-1}	Form I	Form II
Coulombic	-41.8	-37.5
Polarisation	-15.8	-15.2
Dispersion	-163.1	-165.0
Repulsive	95.0	96.6
Cell Dipole	-1.1	0.0
Total	-126.7	-121.2

Table S3| CLP-PIXEL energies (kJ.mol^{-1}) for Form I based on B3LYP/6-31G(d,p) charge densities, showing Coulombic (E_C), Polarization (E_P), Dispersion (E_D), Repulsive (E_R) and total energy (E_{tot}).

Symmetry	Distance	E_C	E_P	E_D	$E_{R.}$	E_{tot}
-x,-y,z+0.5	28.47	0	0	0	0	0
-x+0.5,y,z+0.5	16.258	0	0	-0.2	0	-0.3
x+0.5,-y,z	12.896	-2.2	-0.7	-8.5	4.2	-7.2
x,y-3,z	11.621	0.1	0	-0.2	0	-0.1
x,y-2,z	7.747	0.4	0	-1.4	0	-1.1
x,y-1,z-1	12.594	-0.1	0	-0.2	0	-0.3
x,y-1,z	3.874	-7.6	-5	-68.8	43.4	-37.9
x,y-1,z+1	12.594	0.1	0	-0.1	0	0
x,y,z-1	11.983	-0.1	0	-0.2	0	-0.3
x,y,z+1	11.983	-0.1	0	-0.2	0	-0.3
x,y+1,z-1	12.594	0.1	0	-0.1	0	0
x,y+1,z	3.874	-7.6	-5	-68.8	43.4	-37.9
x,y+1,z+1	12.594	-0.1	0	-0.2	0	-0.3
x,y+2,z	7.747	0.4	0	-1.4	0	-1.1
x,y+3,z	11.621	0.1	0	-0.2	0	-0.1
-x+1,-y-2,z-0.5	12.475	0.1	0	-0.2	0	-0.1
-x+1,-y-2,z+0.5	12.475	0.1	0	-0.2	0	-0.1
-x+1,-y-1,z-0.5	9.391	0.1	0	-1.4	0	-1.4
-x+1,-y-1,z+0.5	9.391	0.1	0	-1.4	0	-1.4
-x+1,-y,z-0.5	7.125	-12	-4.4	-27	16.2	-27.2
-x+1,-y,z+0.5	7.125	-12	-4.4	-27	16.2	-27.2
-x+1,-y+1,z-0.5	6.584	-12.4	-4.1	-27.5	15.8	-28.2
-x+1,-y+1,z+0.5	6.584	-12.4	-4.1	-27.5	15.8	-28.2
-x+1,-y+2,z-0.5	8.12	-0.5	-0.1	-1.4	0	-2
-x+1,-y+2,z+0.5	8.12	-0.5	-0.1	-1.4	0	-2
-x+1,-y+3,z-0.5	10.887	-0.2	0	-0.2	0	-0.4
-x+1,-y+3,z+0.5	10.887	-0.2	0	-0.2	0	-0.4
-x+1.5,y-1,z-0.5	12.301	-2.3	-1.3	-5.6	3.5	-5.7
-x+1.5,y-1,z+0.5	12.301	0.3	0	-0.7	0	-0.5
-x+1.5,y,z-0.5	11.675	-2.8	-1.3	-9	6.6	-6.5
-x+1.5,y,z+0.5	11.675	-2.8	-1.3	-9	6.6	-6.5
-x+1.5,y+1,z-0.5	12.301	0.3	0	-0.7	0	-0.5
-x+1.5,y+1,z+0.5	12.301	-2.3	-1.3	-5.6	3.5	-5.7
x-0.5,-y-1,z	14.274	0	0	-0.5	0	-0.5
x-0.5,-y,z	12.896	-2.2	-0.7	-8.5	4.2	-7.2
x-0.5,-y+1,z	12.605	-2.5	-1.6	-9.4	5.2	-8.3
x-0.5,-y+2,z	13.472	-0.2	-0.1	-0.6	0	-0.8
x-0.5,-y-1,z	14.274	0	0	-0.5	0	-0.5
x-0.5,-y+1,z	12.605	-2.5	-1.6	-9.4	5.2	-8.3
x-0.5,-y+2,z	13.472	-0.2	-0.1	-0.6	0	-0.8

Table S4| CLP-PIXEL energies (kJ.mol^{-1}) for Form II based on B3LYP/6-31G(d,p) charge densities, showing Coulombic (E_C), Polarization (E_P), Dispersion (E_D), Repulsive (E_R) and total energy (E_{tot}).

Symmetry	Distance	E_C	E_P	E_D	$E_{R.}$	E_{tot}
-x, y+0.5, -z+0.5	11.444	-0.3	-0.0	-0.7	0.0	-1.0
-x, -y, -z	21.857	0	0	0	0	0
x, -y+0.5, z+0.5	12.698	0	0	-0.6	0	-0.6
x-3, y, z	13.319	0.2	0	-0.1	0	0
x-2, y, z	8.880	0.4	0	-1.6	0	-1.3
x-1, y, z	4.440	-11.4	-5.4	-72.1	48.2	-40.7
x, y, z-1	13.896	-0.2	0	-0.1	0	-0.3
x, y, z+1	13.896	-0.2	0	-0.1	0	-0.3
x+1, y, z	4.440	-11.4	-5.4	-72.1	48.2	-40.7
x+2, y, z	8.880	0.4	0	-1.6	0	-1.3
x+3, y, z	13.319	0.2	0	-0.1	0	0
-x-1, y-0.5, -z+0.5	14.374	-0.1	0	0.1	0	-0.2
-x-1, y+0.5, -z+0.5	14.374	-0.1	0	0.1	0	-0.2
-x, y-0.5, -z+0.5	11.444	-0.3	0	-0.7	0	-1.0
-x+1, y-0.5, -z+0.5	9.733	-4.8	-2.7	-17.3	10.6	-14.2
-x+1, y+0.5, -z+0.5	9.733	-4.8	-2.7	-17.3	10.6	-14.2
-x+2, y-0.5, -z+0.5	9.896	-2.8	-1.4	-13.1	6.0	-11.2
-x+2, y+0.5, -z+0.5	9.896	-2.8	-1.4	-13.1	6.0	-11.2
-x+3, y-0.5, -z+0.5	11.856	-0.5	0	-0.6	0	-1.1
-x+3, y+0.5, -z+0.5	11.856	-0.5	0	-0.6	0	-1.1
-x-1, -y-1, -z	12.120	0	0	-0.2	0	-0.2
-x-1, -y+1, -z+1	13.588	0.3	0	-0.6	0	-0.3
-x, -y+1, -z	8.578	0.6	-0.1	-1.2	0	-0.7
-x, -y+1, -z+1	10.327	-2.5	-0.7	-11.8	4.6	-10.4
-x+1, -y+1, -z	6.302	-9.3	-5.0	-24.3	15.6	-23.1
-x+1, -y+1, -z+1	8.251	-12.2	-5.5	-33.7	24.3	-27.1
-x+2, -y+1, -z	6.727	-7.4	-3.1	-18.0	8.1	-20.5
-x+2, -y+1, -z+1	8.303	1.4	-0.7	-10.0	4.7	-4.6
-x+3,-y+1,-z+0	9.499	-0.9	-0.1	-1.0	0	-2.0
-x+3,-y+1,-z+1	10.450	0.2	0	-0.5	0	-0.4
-x+4,-y+1,-z+1	13.745	0	0	-0.1	0	-0.1
x-1,-y+0.5,z-0.5	13.364	-0.1	0	-0.2	0	-0.3
x-1,-y+0.5,z+0.5	13.539	0.1	0	-0.3	0	-0.2
x-1.0,-y+1.5,z-0.5	11.659	-0.1	-0.1	-0.9	0	-1.1
x-1,-y+1.5,z+0.5	11.859	-0.6	-0.1	-0.6	0.0	-1.3
x,-y+0.5,z-0.5	12.698	0	0	-0.6	0	-0.6
x,-y+1.5,z-0.5	10.889	-2.2	-1.2	-6.0	3.1	-6.2
x,-y+1.5,z+0.5	10.889	-2.2	-1.2	-6.0	3.1	-6.2
x+1,-y+0.5,z-0.5	13.539	0.1	0	-0.3	0	-0.2
x+1,-y+0.5,z+0.5	13.364	-0.1	0	-0.2	0	-0.3
x+1,-y+1.5,z-0.5	11.859	-0.6	-0.1	-0.6	0	-1.3
x+1,-y+1.5,z+0.5	11.659	-0.1	-0.1	-0.9	0	-1.1

Luminescence Properties

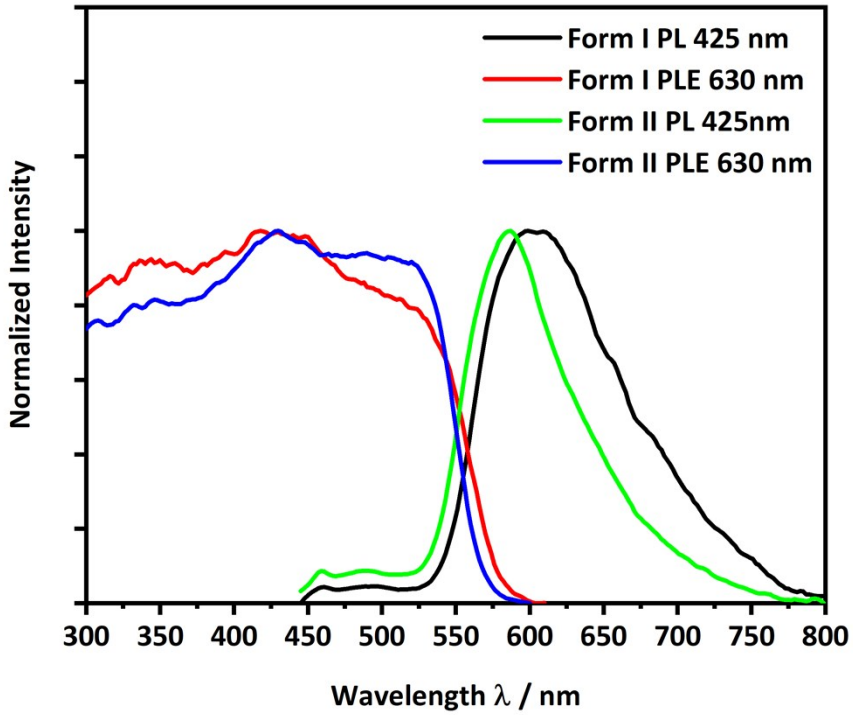

Fig. S8 Solid-state photoluminescence (PL, black line Form I, green line Form II) and photoluminescence excitation (PLE, red line Form I, blue line Form II) spectra of Form I and Form II of CPMBP crystals. For the PLE measurements, only the emission signal at 630 nm was detected and the excitation wavelengths were scanned. The intensity of the signal at 630 nm was then plotted against the excitation wavelength. From the maximum of the PLE measurements we obtain the best excitation wavelength of the photoluminescence.

Theoretical Study

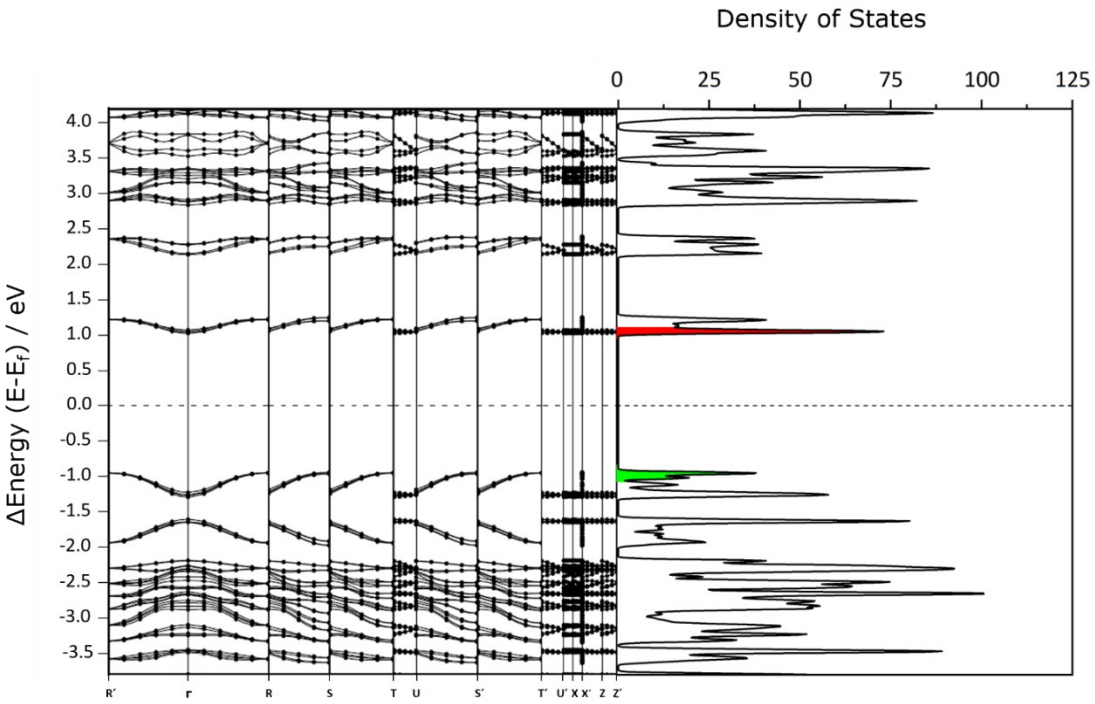

Fig. S9 Band structure and density of states of Form I of CPMBP. The conduction band is highlighted in red and the valence band in green. The corresponding integrals are 2.77 for the valence band and 4.35 for the conduction band.

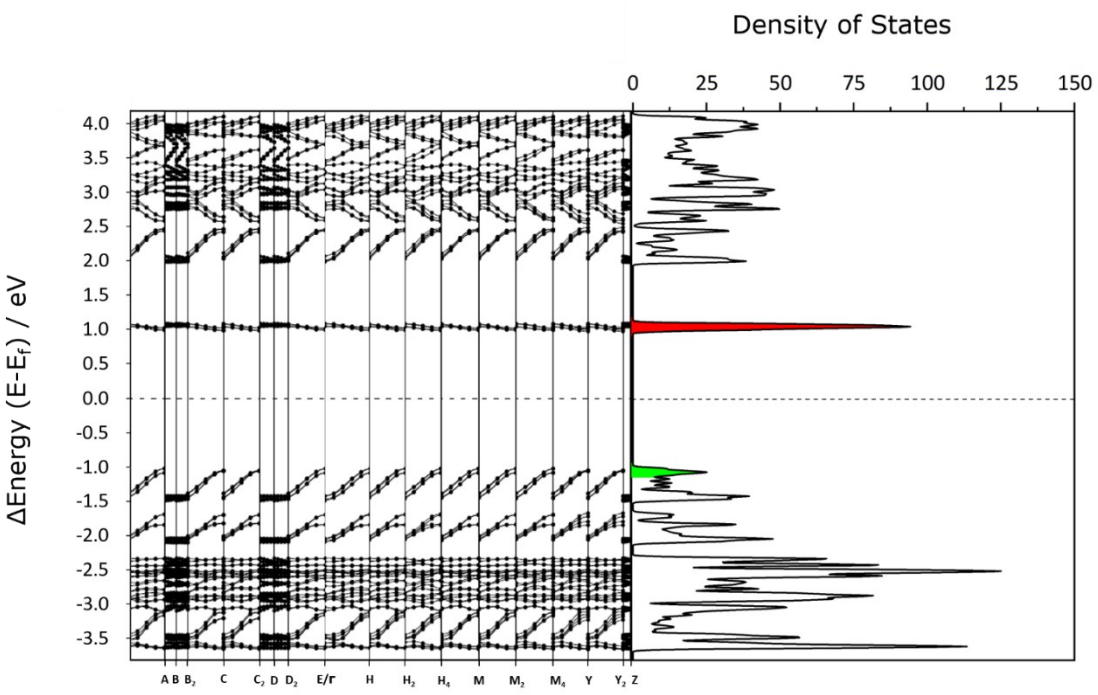

Fig. S10 Band structure and density of states of Form II of CPMBP. The conduction band is highlighted in red and the valence band in green. The corresponding integrals are 2.22 for the valence band and 8.00 for the conduction band.

Optical Waveguiding Study

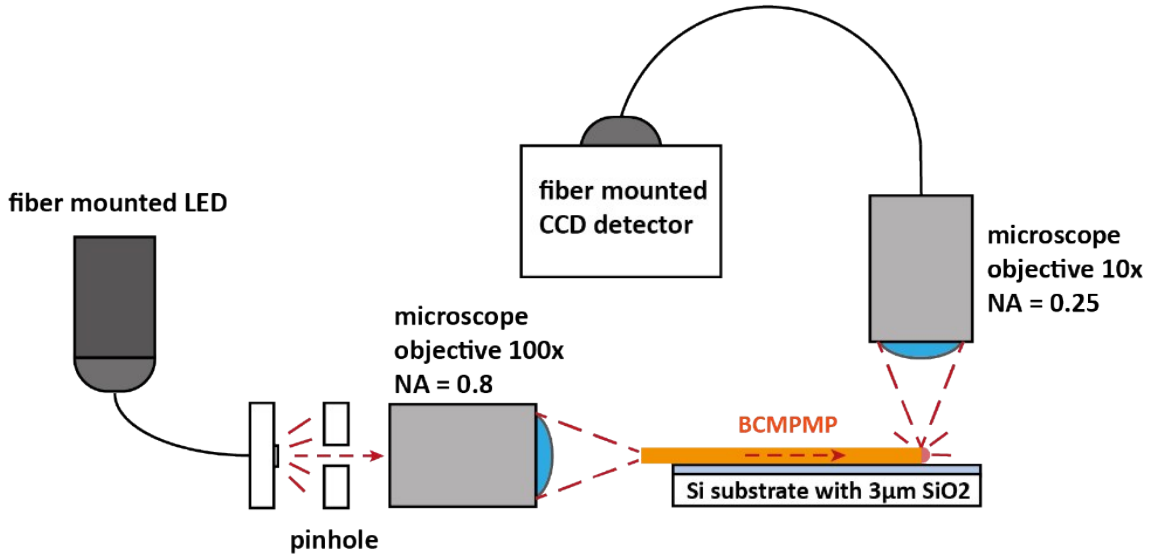

Scheme S1. Schematic representation of the waveguide measurement setup. The sample (CPMBP) was placed on a silicon wafer (3 µm thick SiO2 layer). The LED light was coupled into the sample through a microscope objective (100x magnification, 0.8 numeric aperture (NA). The outcoupled light was detected perpendicular to the optical axis of the waveguide using a microscope objective (10x magnification, 0.25 numeric aperture (NA).

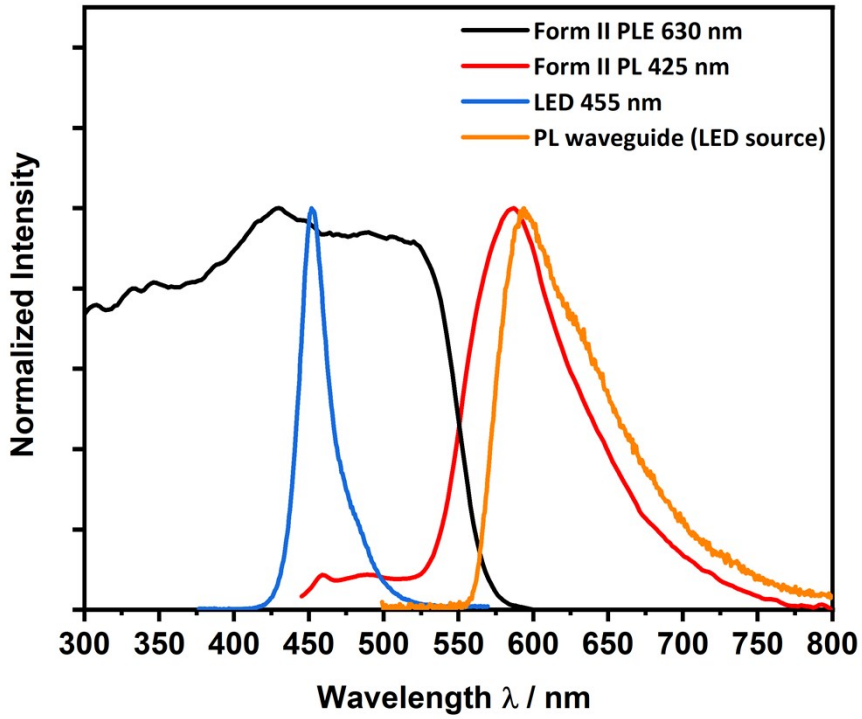

Fig. S11 Solid-state photoluminescence (PL, red line) and photoluminescence excitation (PLE, black line) spectra of Form II together with the spectra of the LED source (455 nm, blue line) and the outcoupled light from the crystal (orange line)

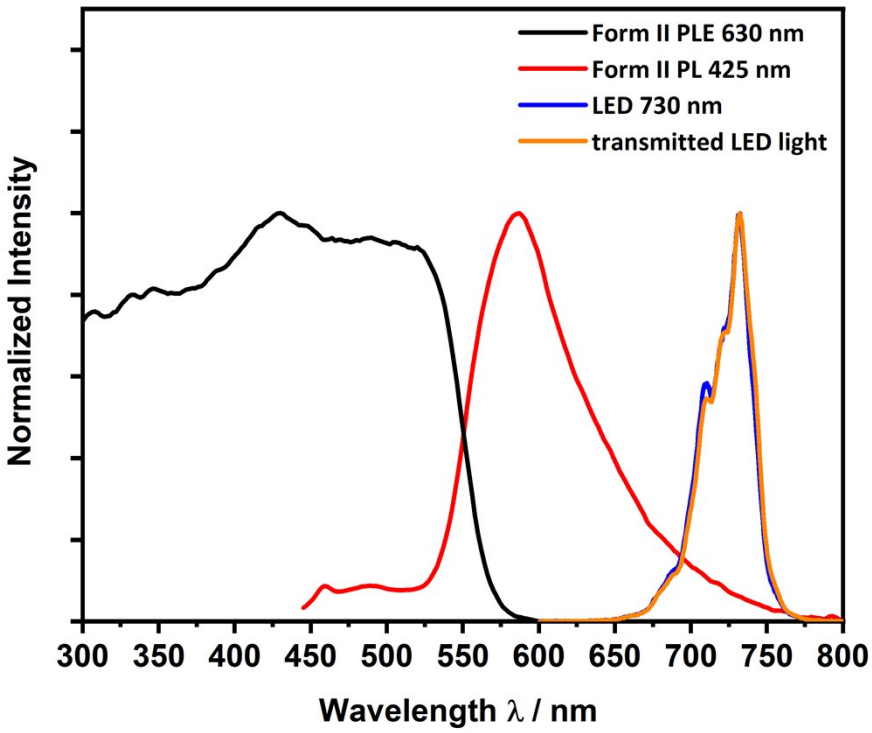

Fig. S12 Solid-state photoluminescence (PL, red line) and photoluminescence excitation (PLE, black line) spectra of Form II together with the spectra of the LED source (730 nm, blue line) and the outcoupled light from the crystal (orange line)

References

1 C. M. Reddy, G. Rama Krishna and S. Ghosh, *CrystEngComm*, 2010, **12**, 2296.
2 K. B. Raju, S. Ranjan, V. S. Vishnu, M. Bhattacharya, B. Bhattacharya, A. K. Mukhopadhyay and C. M. Reddy, *Crystal Growth & Design*, 2018, **18**, 3927–3937.
3 G. R. Krishna, R. Devarapalli, G. Lal and C. M. Reddy, *J. Am. Chem. Soc.*, 2016, **138**, 13561–13567.
4 M. A. Spackman and D. Jayatilaka, *CrystEngComm*, 2009, **11**, 19–32.
5 P. R. Spackman, M. J. Turner, J. J. McKinnon, S. K. Wolff, D. J. Grimwood, D. Jayatilaka and M. A. Spackman, *J Appl Crystallogr*, 2021, **54**, 1–6.